Article:
Matheny-Rabun, C., Holloway, L., Corning, K. et al. (2026) Genetic variants in Rps4x cause intellectual disability with dysmorphic features, microcephaly, and autism. npj Genomic Medicine, 11 (1). 36. ISSN: 2056-7944

https://doi.org/10.1038/s41525-026-00573-0

npj | genomic medicine

Article

Published in partnership with CEGMR, King Abdulaziz University

https://doi.org/10.1038/s41525-026-00573-0

Genetic variants in *Rps4x* cause intellectual disability with dysmorphic features, microcephaly, and autism

Courtney Matheny-Rabun[1], Lynda Holloway[1], Ken Corning[2], Raymond Louie[3], PoNien Lu[1], Thomas Smol[4], Simon Boussion[4], Emily Woods[5], Diana Johnson[5], Catherine Williams[6], Richard Steet[1], Michael Friez[3], Gavin Arno[1], Roger Stevenson[1] & Heather Flanagan-Steet[1] ✉

X-linked intellectual disability (XLID) comprises a group of heterogeneous disorders associated with impaired cognitive function and developmental delays. It has been estimated that 10% of the genes on the X-chromosome are associated with at least one form of intellectual disability. To date, genetic variants in 172 genes have been associated with XLID. Clinically, these disorders are highly variable, with some exhibiting multi-system involvement and others limited only to intellectual impairment. Here we describe a new XLID condition caused by defects in *RPS4X*, which encodes a component of the small (40S) subunit of the ribosome. Genetic testing of two male siblings with dysmorphic facial features, microcephaly, global developmental delay, and autism revealed a maternally inherited missense variant in *RPS4X*. Studies in patient fibroblasts and zebrafish indicate this *RPS4X* variant is pathogenic, with functional findings consistent with the clinical presentation. Four additional individuals with intellectual disability were identified through the GeneMatcher and the 100,000 Genomes project that also bear *RPS4X* variants. Together, these data support *RPS4X* as a new XLID-associated gene, expanding the involvement of ribosomal components in genetic disease.

X-linked intellectual disability (XLID) comprises a clinically and genetically heterogeneous collection of disorders with cognitive impairment and developmental delay caused by variants in genes on the X-chromosome. Currently, genetic variants in more than 170 genes are known to cause XLID, but it is estimated that 10% of the genes on the X-chromosome may be associated with XLID[1]. These disorders are clinically variable, with some exhibiting multi-system involvement and others limited only to intellectual impairment. Genetic mapping studies have identified several X-linked genes related to ribosomal function and biogenesis[2]. Copy number and missense variants in two X-linked ribosomal genes, *RPL10* and *RPS6KA3*, have previously been associated with intellectual disability[3,4].

The ribosome is a large multi-subunit molecular machine comprised of one large (60S) and one small (40S) subunit. In eukaryotes, the small subunit, which contains ~33 proteins and a single rRNA, recognizes and binds messenger RNAs. The large subunit comprises ~49 proteins and 3 rRNAs that catalyze the formation of peptide bonds[5]. Decades of research have suggested that ribosomal assembly exclusively occurs in the nucleolus. This model proposes that ribosomal proteins are synthesized in the cytosol and subsequently imported into the nucleolus. Here, along with locally transcribed rRNAs, they are assembled into their respective subunits. Recent studies describe a much more dynamic process that challenges this long-standing dogma[6]. While the conventional view of the ribosome depicts a single static complex, it is increasingly evident that surface ribosomal proteins can be locally synthesized and incorporated into existing ribosomes in situ. This mechanism, which is particularly prevalent within neuronal synapses, remodels ribosomes into specialized machines optimized for specific protein products. A recent study performed in cultured neurons identified a loop-forming motif in the 5'UTR of several mRNAs that controls the subcellular synthesis of certain ribosomal proteins[7]. This study showed that synapse-localized synthesis of the multiple ribosomal proteins, including the small 40S subunit component RPS4X, depend on this element and disruptions in RPS4X synthesis disrupt neuron dendrite formation. Of the ribosomal proteins surveyed in this study, *RPS4X* exhibited the highest increase in expression during chemofactor-induced axon growth. These

[1]JC Self Research Institute Greenwood Genetic Center, Greenwood, SC, USA. [2]Greenwood Genetic Center, Columbia Office, Columbia, SC, USA. [3]Diagnostic Laboratories, Greenwood Genetic Center, Greenwood, SC, USA. [4]Univ. Lille, ULR7364 - RADEME - Maladies RAres du DEveloppement embryonnaire et du Métabolisme, Lille, France. [5]Sheffield Clinical Genetics Service, Sheffield Children's Hospital NHS Foundation Trust, Sheffield, UK. [6]Royal Wolverhampton Hospital NHS Trust, Wolverhampton, UK. ✉e-mail: heatherfs@ggc.org

data highlight the importance of local ribosomal remodeling in neuronal development and identify a role for RPS4X during axon outgrowth and establishment of neuronal circuitry.

Here we report three male individuals with global developmental delay and intellectual disability, who each harbor a rare or previously unreported missense variant in *RPS4X*. Additional clinical findings included autism, dysmorphic facial features, microcephaly and ectopic pituitary. Included are two male siblings carrying a maternally inherited missense variant and an unrelated individual with an *RPS4X* variant identified through GeneMatcher. Eleven additional individuals were identified in the Genomics England 100,000 genomes project (100KGP). Functional studies performed in cells isolated from two individuals support the pathogenicity of a subset of these variants. This designation is further strengthened by studies in zebrafish, which demonstrate the need for normal Rps4x function during early brain development. Together, our data implicate *RPS4X* as a potential new XLID gene and add to the growing body of evidence supporting the important contributions of several small ribosomal proteins during early neuronal development.

Results

Clinical findings

Two male siblings were first seen at the GGC in 2001 for suspicion of a genetic condition associated with dysmorphic facial features, microcephaly, and global developmental delay (Supplementary Fig. S1). For both individuals, a flat midface, long smooth philtrum, thin upper lip, small ears with over folded helices, and horizontal palmar creases were also noted. Hypotonia was noted in both brothers in infancy, with brain MRIs performed in infancy also identifying periventricular leukomalacia and frontal lobe atrophy. By age 9 the older brother (individual 1, I1) was found to have an ectopic pituitary gland, an increasingly prominent jaw, and was diagnosed with attention-deficit hyperactivity disorder (ADHD) and autism spectrum disorder (ASD). Similarly, during childhood the younger brother (individual 2, I2) was shown to have a posterior placed pituitary gland and was also diagnosed with ADHD and ASD. Both individuals exhibit intellectual disability.

Genetic studies

Extensive clinical genetic testing, including chromosome and microarray analyses, targeted Sanger sequencing of multiple genes associated with XLID, DNA methylation analysis, and biochemical assessment of plasma amino acid and organic acid levels, were previously performed. All tests were considered uninformative. As part of this study, reanalysis of existing exome sequencing data was performed. A maternally inherited missense c.662G>A, p.(Arg221Gln) variant of uncertain significance in the *RPS4X* gene was identified in both affected siblings (Fig. 1 and Table 1). Other variants identified included a c.842C>A;p.(Ala281Glu) in *ZMAT1* and a c.8332G>A;p.(Gly2778Arg) in *MRXA5*. Neither of these variants segregated with clinical disease in this family. No candidate biallelic autosomal variants shared by both siblings were identified, and no other compelling variants were identified on the X chromosome. X-inactivation studies across the family showed inactivation was preferentially skewed toward one chromosome (ranging from 89:11 to 98:2) in all women carrying the p.(Arg221Gln) *RPS4X* alteration (Fig. 1A). The *RPS4X* coding region is present at Xq13.1, and although it escapes X-inactivation it is closely opposed to the X-inactivation regulator, *X-IST*[8]. An *RPS4X* paralogue (*RPS4Y*), which shares 93% homology with *RPS4X*, is present on the Y chromosome (Fig. 1B). The two proteins are not identical, but studies in cells and in mice show they can functionally compensate for one another[9].

Additional *RPS4X* variants identified in individuals through the GeneMatcher and Genomics England databases. Additional patients bearing rare variants in *RPS4X* were identified through the Gene Matcher matchmaking portal and the 100KGP dataset. The third individual (I3), identified via Gene Matcher[10], a 3-year-old male affected by intrauterine growth restriction (IUGR), mild facial dysmorphism, developmental and speech delays, as well as ADHD and intellectual disability, harbors a maternally inherited hemizygous frameshift c.755_758delGAGA;-p.(Arg252ThrfsTer26) in *RPS4X* (see Table 1). This variant, which is located in the final exon of the gene, is predicted to cause frame shift in the 3' end of the transcript that could alter the C-terminus of RPS4X. Four additional unrelated individuals with intellectual disability that also harbor rare missense *RPS4X* variants were identified in the Genomics England Database (see Table 2, individual 4–7). Individual 4 is a male born to non-consanguineous parents, who has intellectual disability. Like individuals 1 and 2, individual 4 also has an ectopic posterior pituitary gland. He was found to harbor a rare maternally inherited *RPS4X* variant, c.712C>T, p.(Leu238Phe), seen in three individuals in the gnomAD v4.1.1 dataset (including a single hemizygote). The p.(Leu238Phe) variant was found in one additional family in the 100KGP dataset (Table 2, individual 5) with intellectual disability and developmental delay among his clinical features. This individual was also found to harbor a de novo frameshift variant in the *KAT6A* gene (c.2218delC;p.Arg740ValfsTer6). The presence of this second variant makes it difficult to determine if the *RPS4X* variant also contributes to his disease. It is not known if dual pathology (*KAT6A*-syndrome and *RPS4X*) is responsible for the clinical constellation and follow up is not possible. Individual 6 is a male and the only child of non-consanguineous parents, who has intellectual disability, ASD, global developmental delay and abnormal skull morphology. Following negative clinical interrogation of his genome, including genes implicated in congenital disorders of glycosylation, RASopathy and intellectual disability, reanalysis of the data revealed a missense variant, c.770C>T, p.(Ala257Val) in the *RPS4X* gene. This variant is absent from gnomAD v2, as well as any other family in the 100KGP. The variant is observed in 9/1,208,084 alleles in gnomAD v4.1 including two hemizygotes, although these variant calls failed quality filters. Individual 7 is a male and the only child born to non-consanguineous parents, was diagnosed with intellectual disability, delayed gross and fine motor development, global developmental delay, delayed speech and language development, ASD and failure to thrive. His developmental delay was

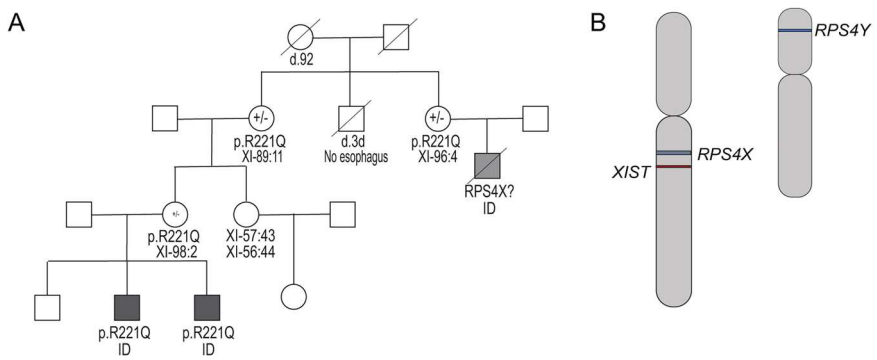

Fig. 1 | de novo variants in *RPS4X* co-segregate with intellectual disability in males from a multi-generational family. A A multi-generational pedigree shows two males siblings with intellectual disability carry the p.(Arg221Gln) RPS4X variant, with all female carriers exhibiting skewed X-inactivation. Unaffected males do not carry the variant. Testing was not possible in the deceased affected uncle. **B** Schematic of the X- and Y chromosomes denote the location of *RPS4X* (relative to the X-IST loci) and *RPS4Y*.

Table 1 | Summary of clinical features for 3 individuals with *RPS4X* variants

Individual gender	1 male	2 male	3 male
Clinical presentations	DD DLD ASD/ADHD MRI identified PVL Microcephaly Dysmorphic Facies Ectopic pituitary	DD DLD ASD/ADHD MRI identified PVL Microcephaly Dysmorphic Facies, Ectopic pituitary	IUGR ID DD DLD ADHD Mild facial dysmorphism
Variant-cDNA	c.662G>A	c.662G>A	c.755_758delGAGA
Variant- protein	p.(Arg221Gln)	p.(Arg221Gln)	p.(Arg252ThrfsTer26)
Family members sequenced	Mother Affected sib (I2)	Mother Affected sib (I1)	Mother
Inheritance	maternal	maternal	maternal
Zygosity	hemizygous	hemizygous	hemizygous
Alpha missense prediction	0.9897 Pathogenic	0.9897 Pathogenic	NA
REVEL	0.79	0.79	NA
gnomAD MAF	0	0	0
Other findings	*ZMAT1* c.842C>A;p.(Ala281Glu) *MRXA5* c.8332G>A;p.(Gly2778Arg)	*ZMAT1* c.842C>A;p.(Ala281Glu) *MRXA5* c.8332G>A;p.(Gly2778Arg)	None

DD Developmental Delay, *DLD* Developmental Language Disorder, *PVL* periventricular Leukomalacia, *ASD* Autism Spectrum Disorder, *ADHD* Attention Deficit Hyperactivity Disorder, *IUGR* Intrauterine Growth Restriction, *ID* Intellectual disability, *MAF* Minor Allele Frequency, *VUS* Variant of Uncertain Significance.

first noted at age 16 months. Physical examination at that time showed height and weight at below 0.4th centile with occipitofrontal circumference in the 25th centile. He was noted to have some café au lait patches, mild dysmorphic facies, pectus excavatum, pes planus and clinodactyly. An MRI performed at 2 years old showed white matter lesions and minor periventricular white matter hyperintensities. Reanalysis of the rare variant data following negative clinical interrogation, identified a missense variant, c.282G>T, p.(Lys94Asn) in the *RPS4X* gene. This variant was also absent from the gnomAD v4.1 dataset and all other families in the 100KGP.

From a survey of the 100KGP data, seven additional individuals were identified who harbor rare missense variants in *RPS4X* with limited evidence of pathogenicity (see Table 2, I8-14). Of these, individuals 8, 9, and 11–13 carried missense variants that are predicted to be benign by AlphaMissense. However, two variants, the p.(Asn179Lys) and p.(Arg113Cys) noted in individuals 10 and 14, are predicted by AlphaMissense to be pathogenic. Individuals 9 and 10 had a family history not typical for X-linked disease. Individuals 8, 9, 11, and 12 were not affected by ID/DD spectrum disorders and individual 14 is female. We do not exclude the possibility that some of these variants are disease associated and therefore presented them here. We acknowledge that some of these variants may act via a different mechanism with different phenotypic outcomes.

Bioinformatic data suggest RPS4X may be intolerant to most loss-of-function variants. RPS4X is highly conserved among vertebrate species. Protein alignment shows 100% conservation across the coding regions of a small number of vertebrate species, with the exception of zebrafish, which is 94% identical to human *RPS4X* (Fig. 2A). This suggests that many residues may be intolerant to loss function. This is further supported by the protein tolerance landscape. With the exception of the p.(Leu238Phe) variant, all of the variants reported here reside in regions largely predicted to be intolerant to loss of function (Fig. 2B). In fact, only one predicted loss of function *RPS4X* variant exists in the gnomAD v4.1 dataset, c.781_782delAG, p.(Ser261GlnfsTer9). Like individual 3 reported here, the p.(Ser261GlnfsTer9) variant is predicted to cause a frameshift alteration at the 3' end (codon 261 of 264) of the gene, which could alter the c-terminus of RPS4X. Since this variant is located in the final exon of the gene it is predicted to evade nonsense-mediated decay (NMD) and cause a frame shift in the 3' end of the transcript. However, without directly testing this possibility it cannot be excluded that the resulting transcript would be degraded. The absence of any other coding LOF variants in population data is consistent with the possibility that this gene may be essential. If true, severe disruption of RPS4X may be incompatible with life. This possibility is yet to be proven, however. No variant constraint data are currently available in gnomAD v4.1, although the most common protein-altering variant is only found in 65 of 1.2 M alleles in gnomAD v4.1 and there is a single predicted loss-of-function allele (p.Ser261GlnfsTer9), which is a frameshift variant in the final exon. The probability of loss-of-function intolerance for RPS4X in gnomAD v2 is 0.93 with an observed/expected ratio of 0. Together, the data suggest a low rate of gene variation. Seven missense variants of uncertain significance are reported in ClinVar. The AlphaMissense tool suggests 5 of the variants reported here are damaging, predicting them to be pathogenic (Tables 1 and 3) Only one variant, the p.(Ala257Val) was considered ambiguous (Fig. 2C). Notably, AlphaMissense predicts most variants across the *RPS4X* coding sequence to be pathogenic. Given the high degree of conservation among vertebrate species, it is unclear whether these predictions are accurate, or if they are skewed by over weighting of amino acid conservation as a parameter. The predicted structure of RPS4X indicates each of the variants reported in this study reside on external-facing domains of the protein (Fig. 2D). It is plausible that these variants cause intrinsic protein instability, but their location in these outward-facing regions could instead disrupt interactions between RPS4X and other components of the 40S ribosomal subunit. Although not tested in the current study, we hypothesize that this could compromise local incorporation of RPS4X into the ribosome increasing its proteolysis.

Functional studies

Reduced abundance of the RPS4X^{R221Q} protein is associated with abnormal brain development. Studies in patient fibroblasts and zebrafish further support the p.(Arg221Gln) *RPS4X* variant as pathogenic, with functional findings consistent with the clinical presentation of individuals 1 and 2. Western blot analyses of RPS4X abundance showed a ~ 30% reduction in affected patients compared to male controls. This was true in fibroblasts isolated from the original affected male proband compared either to his unaffected male sibling or an unrelated male control (Fig. 3A, B and Supplementary Fig. S2A, B). Reduced RPS4X

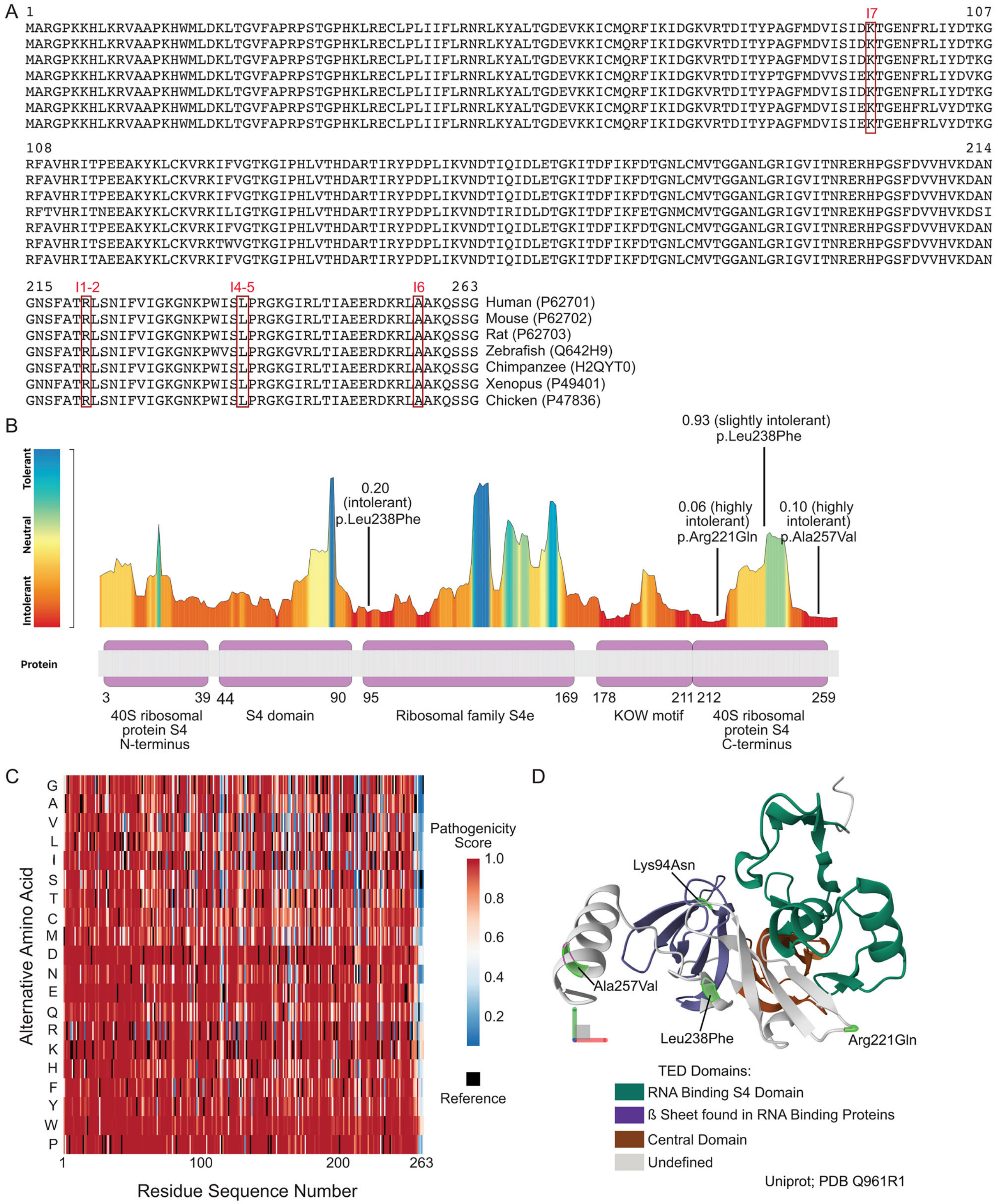

Fig. 2 | The RPS4X missense variants found in individuals 1–6 are predicted to be pathogenic. **A** Alignment of RPS4X sequences from multiple vertebrate organisms show a high degree of conservation. **B** Protein tolerance landscape show the 4 variants reported here occur in important functional domains and regions intolerant to variation[12]. Landscape image exported from https://stuart.radboudumc.nl/metadome/method. **C** The Alpha Missense tool predicts most variants across the coding sequence to be pathogenic. **D** The schematic represents the predicted protein structure of RPS4X with the reported variants indicated. This suggests the variants are all present in outward-facing regions of functional domains. The Encyclopedia of Domains[13] domains are highlighted. Protein structure was exported from Uniprot; AlphaFold DB Q96IR1.

Table 2 | Summary of additional individuals with *RPS4X* variants not consistent with this study

Individuals Gender	I4 male	I5 male	I6 male	I7 male	I8 male	I9 male	I10 male	I11 male	I12 male	I13 male	I14 female
Clinical presentations	ID Ectopic pituitary	ID DD Failure to thrive Abnormality of brain morphology Hypotonia Short stature Abnormal digit morphology	DD ASD Abnormal skull morphology	ID DD DLD ASD Failure to thrive Mild facial dysmorphism Short stature Pes planus Pectus excavatum Clinodactyly c.282G>T	Renal agenesis	Ataxia tremor	ID DD	Absence seizures Infantile spasms EEG abnormality	Nephrocalcinosis Hypercalciuria Nephrolithiaisis	ID Infantile spasms Seizures	ID DD Seizures
Variant-cDNA	c.712C>T	c.712C>T	c.770C>T	c.282G>T	c.682A>G	c.622G>A	c.537C>G	c.536A>G	c.508A>G	c.239T>A	c.337C>T
Variant- protein	p.(Leu238Phe)	p.(Leu238Phe)	p.(Ala257Val)	p.(Lys94Asn)	p.(Ile228Val)	p.(Val208Ile)	p.(Asn179Lys)	p.(Asn179Ser)	p.(Thr170Ala)	p.(Ile80Val)	p.(Arg113Cys)
Family history	Mother Father	None	Mother	Mother Father	None	Dominant (non-segregating)	Affected female sibling	None	None	None	None
Inheritance	Maternal	Maternal	Maternal	Maternal hemizygous	Unknown	Maternal	Maternal	Maternal	Unknown	Maternal	Unknown
Zygosity	Hemizygous	Hemizygous	Hemizygous	Hemizygous	Hemizygous	Hemizygous	Hemizygous	Hemizygous	Hemizygous	Hemizygous	Heterozygous
Alpha missense prediction	0.9133 likely pathogenic	Likely pathogenic	s 0.3488 ambiguous	0.9777 likely pathogenic	Benign	Benign	Pathogenic	Benign	Benign	Benign	Pathogenic
REVEL	0.241	0.241	0.115	0.34	0.54	0.09	0.55		0.48	0.05	0.69
gnomAD MAF	0.000004478	0.000004478 1 hemizygote	0	0	0.00005917 1 hemizygote	0	0	0.00002359	0	0.0000123 3 hemizygotes	0
Other findings	Homoplasmic m.7041G>A, *MT-CO1* p.Val380Ile VUS	c.2218delC p.Arg740ValfsTer6 *KATA6A* VUS	None	None							

Table 3 | Summary of AlphaMissense predictions for each reported variants and other possible variants at the same position

Residue change	AlphaMissense score	Predicted effect	Residue change	AlphaMissense score	Predicted effect	Residue change	AlphaMissense score	Predicted effect	Residue change	AlphaMissense score	Predicted effect
Variants related to I1 and I2			Variants related to I4			Variants related to I5			Variants related to I6		
R221A	0.9953	Pathogenic	L238A	–	–	A257A	NA	NA	K94A	–	–
R221C	0.9939	Pathogenic	L238C	–	–	A257C	–	–	K94C	–	–
R221D	0.9987	Pathogenic	L238D	–	–	A257D	–	–	K94D	–	–
R221E	0.9938	Pathogenic	L238E	–	–	A257E	0.6546	Likely path	K94E	0.944	likely path
R221F	0.9991	Pathogenic	L238F	0.9133	Likely path	A257F	–	–	K94F	–	–
R221G	0.9948	Pathogenic	L238G	–	–	A257G	0.2916	Likely benign	K94G	–	–
R221H	0.9931	Pathogenic	L238H	0.9957	Likely path	A257H	–	–	K94H	–	–
R221I	0.9952	Pathogenic	L238I	0.4216	Ambiguous	A257I	–	–	K94I	–	–
R221K	0.9817	Pathogenic	L238K	–	–	A257K	–	–	K94K	NA	NA
R221L	0.9841	Pathogenic	L238L	NA	NA	A257L	–	–	K94L	–	–
R221M	0.9993	Pathogenic	L238M	–	–	A257M	–	–	K94M	0.9504	likely path
R221N	0.9988	Pathogenic	L238N	–	–	A257N	–	–	K94N	0.9777	likely path
R221P	0.9966	Pathogenic	L238P	0.9901	Likely path	A257P	0.9852	Likely path	K94P	–	–
R221R	NA	NA	L238R	0.9933	–	A257R	–	–	K94R	0.1175	likely benign
R221Q	0.9897	Pathogenic	L238Q	–	–	A257Q	–	–	K94Q	–	–
R221S	0.9983	Pathogenic	L238S	–	–	A257S	0.156	Likely benign	K94Q	0.7022	likely path
R221T	0.9982	Pathogenic	L238T	–	–	A257T	0.3021	Likely benign	K94T	0.9157	likely path
R221V	0.9928	Pathogenic	L238V	0.5335	Ambiguous	A257V	0.3488	Ambiguous	K94V	–	–
R221W	0.9969	Pathogenic	L238W	–	–	A257W	–	–	K94W	–	–
R221Y	0.998	Pathogenic	L238Y	–	–	A257Y	–	–	K94Y	–	–

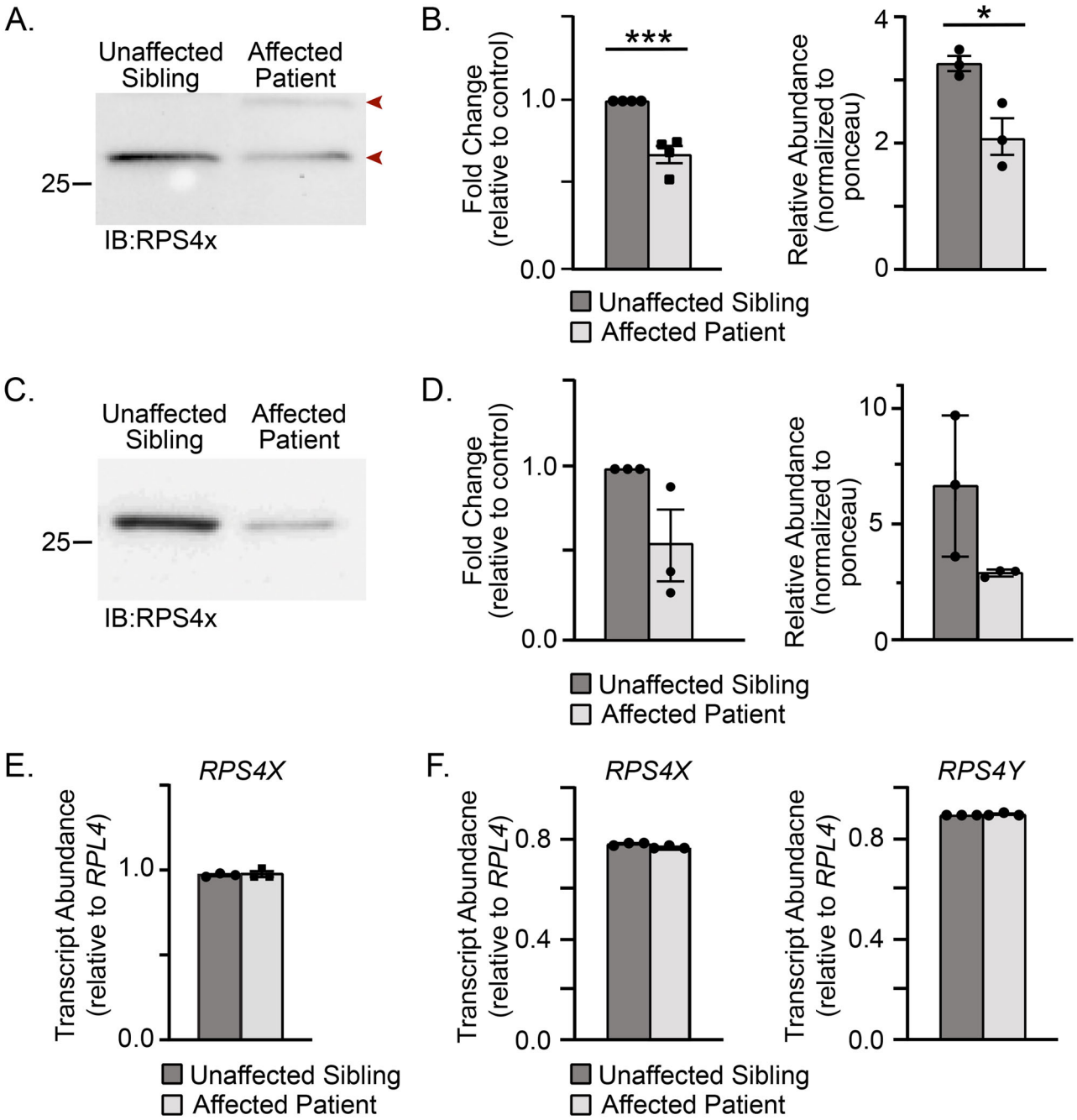

Fig. 3 | RPS4X abundance is reduced in cells from patients carrying the p.(Arg221Gln) variant. A, **B** Western blot analyses of RPS4X in patient derived fibroblasts show protein abundance is reduced ~30% in the affected proband compared to the unaffected male sibling. **C**, **D** Western blot analyses of EBV-transformed lymphoblasts (generated from the proband and his unaffected male sibling) show a similar a reduction in RPS4X abundance. In this case the reduction did not reach statistical significance, likely due to variability in growth of lymphoblasts cultures. **E** Quantitative PCR performed in fibroblasts showed no difference in *RPS4X* transcript abundance between the affected and unaffected male sibling. **F** Similarly quantitative PCR performed on lymphoblasts also showed no difference in the *RPS4X* or *RPS4Y* transcript abundances. For all experiments $n = 3$ biological replicates. Error = S.E.M, Significance was calculated by the Student's *t* test where $^{*}p < 0.05$ and $^{***}p < 0.001$.

abundance was also evident in microscopic images of immunohistochemically stained fibroblasts (Supplementary Fig. S2B). Although more variable and not statistically significant, western blots of EBV-immortalized lymphoblasts similarly suggest RPS4X abundance is reduced by the p.(Arg221Gln) variant (Fig. 3C, D and Supplementary Fig. S2C). The specificity of the RPS4X antibody was validated in western blots of cultured HEK cells transfected with an RPS4X expression plasmid (Supplementary Fig. S2D). Quantitative RT-PCR analyses of transcript abundance in fibroblasts and EBV-transformed lymphoblasts suggest reduced RPS4X protein abundance does not stem from changes in either the *RPS4X* or *RPS4Y* transcript levels (Fig. 3E, F). To ask whether 30% less RPS4X can alter brain development, we used anti-sense morpholinos to transiently reduce *rps4x* expression in developing zebrafish (Fig. 4A–C). Reducing its protein abundance by 30% impaired mid and hindbrain formation in developing embryos (Fig. 4D and Supplementary Fig. S3A). Most importantly, co-injection with either WT *rps4x* mRNA or variant-carrying mRNA showed wild type mRNA (but not variant containing) restores normal brain morphology (Fig. 4E). Expression of

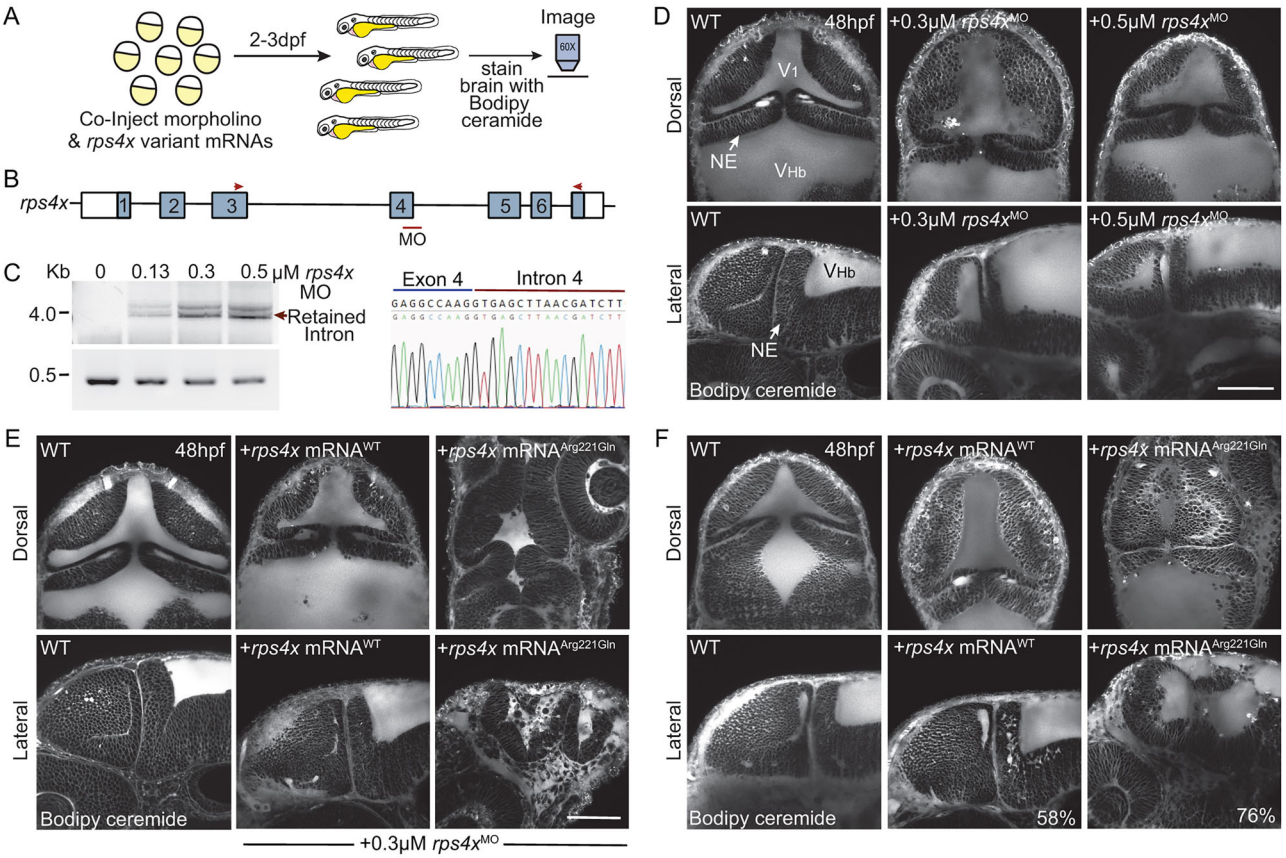

Fig. 4 | A 30% reduction in *rps4x* disrupts brain formation in zebrafish embryos. **A** Schematic shows the workflow for microscopic analysis of morpholino-based inhibition and rescue of rps4x expression. **B** Schematic of the *rps4x* coding region in zebrafish. The position of the splice bocking morpholino is denoted (red line, MO), as is the position of the forward and reverse primers (red arrow heads) used for RT-PCR analysis of knockdown. **C** RT-PCR analysis of *rps4x* transcript in morpholino-injected embryos 48hpf show increased abundance of intron-containing transcripts is associated with lower levels of normal *rps4x* transcript. Based on these data 0.3 μM morpholino reduced normal *rps4x* transcript abundance ~30%. The associated sequencing trace showing retention of intron 4 is shown. **D** Live confocal images of 48hpf embryos stained with BODIPY-ceramide show morpholino inhibition of rps4x disrupts formation of the mid and hindbrain. The ventral hindbrain (VHb), the neuroepithelial fold (NE), and first ventricular space (V1) are labeled. $n = 20–25$ embryos per condition from 3 biological matings. **E** Live images of BODIPY-ceramide stained embryos co-injected with 0.3 M morpholino and either wild type[13] or p.(Arg221Gln) variant containing *rps4x* mRNA shows only WT mRNA improves morphant phenotypes. $n = 15–20$ embryos per condition from 3 biological matings. **F** Live images of BODIPY-ceramide stained wild type embryos injected with either wild type or p.(Arg221Gln) variant containing *rps4x* mRNA show the variant containing mRNA disrupts normal brain development. $n = 18–20$ embryos per condition from 3 biological matings. Percent values indicate number of embryos with the pictured phenotypes. For all images the upper panels represent the dorsal view of the brain and lower panels the ventral view. Scale bar = 10 μM.

either the WT *rps4x or* the p.(Arg221Gln) variant in control embryos also disrupted formation of the mid and hindbrain (Fig. 4F). While increased expression of WT *rps4x* mRNA was mildly damaging, overexpression of the p.(Arg221Gln) variant was highly toxic. In fact, increased levels of this variant caused more severe abnormalities than those associated with reduced *rps4x* expression. Based on data from cultured fibroblasts bearing the p.(Arg221Gln) and the finding that overexpression of wild-type *rps4x* is damaging, we suspect the toxicity relates to a dosage effect. However, we cannot rule out the possibility that the p.(Arg221Gln) has a deleterious dominant effect, like aggregation of unstable protein, as well.

Discussion

Intellectual disability (ID) affects 1–3% of people world-wide. Up to 10% of males diagnosed with intellectual disability bear variants in an X-linked gene. To date 172 different X-linked genes have been associated with ID[1]. Here, we report 7 male individuals from 6 different families with ID who bear variants in *RPS4X*. Studies on one of these variants, p.(Arg221Gln) in patient fibroblasts and zebrafish, support its pathogenic consequence. Western blot analyses of RPS4X abundance in individuals 1 and 2 showed a ~30% reduction compared to male controls. This was true in fibroblasts isolated from the affected proband compared to his unaffected male sibling, and although not statistically significant also in EBV-immortalized lymphoblasts. Consistent with previous studies in Xenopus[7], a 30% reduction in Rps4x abundance impaired mid and hindbrain formation in zebrafish. WT mRNA partially restored brain formation in these animals, but mRNA bearing the p.(Arg221Gln) variant did not.

Five additional individuals, identified through the GeneMatcher and Genomics England 100KGP databases, exhibit a similar constellation of phenotypes with global developmental delay, ADHD/ASD, and intellectual disability being the most evident and consistent features. Like individuals 1 and 2, individuals 3 and 7 also had mild facial dysmorphism. Notably, an ectopic pituitary gland was observed in three individuals. With the exception of the p.(Arg257Val) variant, which was considered ambiguous, the AlphaMissense tool predicts the remaining 4 variants to be pathogenic. Among the variants presented in Table 2, five were predicted to be pathogenic or likely pathogenic by Alphamissense and found in individuals with neurological impairment; individual 5 had *RPS4X* p.Leu238Phe identified in addition to a pathogenic *KAT6A* variant, individual 10 had an affected female sibling and individual 14 is female. Despite their exclusion from the primary group considered in this study, it is plausible that these variants are also contributing to disease. Future studies into the functional impact of these on RPS4X may help

clarify whether RPS4X defects are in fact associated with disease in females. The fact that *RPS4X* escapes X-inactivation may suggest higher expression levels than achieved by hemizygosity may be needed during development. This possibility is supported by the presence of the *RPS4Y* gene. If true, severe variants that significantly alter protein function could compromise neural development in females, with the milder variants primarily affecting males. Analysis of expression in female carriers of the p.Arg221Gln variant may help clarify this possibility and also inform whether RPS4Y expression in males prevents more severe disease.

Together, the clinical and functional data presented here support *RPS4X* deficiency as a cause of XLID. Given the clear association between the *RPS4X* variants identified and the onset of specific neurological phenotypes, these data further strengthen the growing body of evidence that suggest synthesis of certain ribosomal proteins and the associated ribosomal remodeling is essential for normal neural development[11]. It should be noted, however, that our ability to assign pathogenicity to the majority of variants presented here is limited by multiple factors, including the lack of more extensive information on each individual's clinical presentation. Additionally, without samples from each individual and in the absence of a heterologous cellular system to express each variant, we cannot functionally interrogate pathogenicity. Further, it is possible that some variants do not directly impair RPS4X stability but instead inhibit its incorporation into local ribosomes within the nervous system. Investigating this possibility will require an in vitro reconstitution system that is outside the scope of this study. Future studies aimed at defining how these variants impact RPS4X function and mechanistically cause disease are warranted. Despite these limitations, our data in zebrafish showing Rps4x is essential for mid and hindbrain development do support its role in neural development. Similar analyses in Xenopus suggested Rps4x directly influences the level of protein translation in developing axons, further showing that synapse-localized synthesis of RPS4X regulates axonal branching[7]. Our study does not specifically address how these variants impact synapse-localized synthesis, but the finding that RPS4X abundance is reduced in patients with intellectual disability is consistent with this possibility.

Methods

Patient and ethical compliance

Individuals 1 and 2 were seen at the Greenwood Genetic Center for genetic evaluation related to global developmental delay and dysmorphic facial features. In both cases informed consents were signed by the parents of the individuals prior to participation in research studies. This study was reviewed and approved by the Institutional Review Board of Self Memorial Hospital (Greenwood, SC), and compliant with practices at the Greenwood Genetic Center (GGC). Individual 3 was seen for genetic evaluation at Lille University Hospital, France; informed consent was signed by the parents of individual 3 prior to inclusion in this research study. Individuals 4–7 were identified through the interrogation of the rare variant data within the 100KGP, informed consent for genome analysis was obtained in accordance with approval from the HRA committee East of England-Cambridge south (REC 14/EE/1112). This study was performed in accordance with the tenets of the declaration of Helsinki.

Exome sequencing and identification of RPS4X (NM_001007.4) c.622 G > A;p.(Arg221Gln)

ES was performed on the proband, his affected and unaffected brothers, both parents and multiple family members as previously described. The resultant variant data were analyzed as previously described[12]. DNA libraries were prepared from 3 µg of genomic DNA isolated from the proband and parental samples, using the Agilent Clinical Research Exome[13] v1 capture kit (Agilent Technologies, Santa Clara, CA). DNA was fragmented using the Covaris S220 system (Covaris, Woburn, MA), and fragments of 150–200 bp were selected using AMPure XP beads (Beckman Coulter, Brea, CA). Fragments were subsequently end-repaired, adenylated at the 3' end, ligated to sequencing adaptors, and then PCR-amplified using the SureSelect^{XT} Library Preparation kit (Agilent Technologies). DNA was next purified using AMPure XP beads. The concentration of the enriched libraries was determined using a DNA-1000 chip on the 2100 Bioanalyzer (Agilent Technologies). 750 ng of each DNA library was used for hybridization and capture with the CRE v1 probes (Agilent Technologies). After hybridization, the RNA-bound DNA was retained, and unhybridized material was washed away. Captured fragments were amplified by PCR and purified. The quality of the enriched libraries was evaluated using a High-Sensitivity DNA chip on the 2100 Bioanalyzer. Libraries were quantified on a Qubit® 2.0 Fluorometer using a Qubit High Sensitivity kit (Life Technologies, Waltham, MA), and separate libraries were pooled and sequenced using an Illumina NextSeq 500® Sequencing System (Illumina Inc., San Diego, CA) per the manufacturer's protocol. Exome sequencing generated a minimum of 97 million reads per patient sample with an average read length of 75 bp. Sequences were processed using NextGENe software (SoftGenetics, LLC, State College, PA) and trimmed for low-quality and duplicate reads. Reads were trimmed or rejected when the median Phred quality score was below 20 and/or had more than three bases with a Phred score ≤16. The sequences were then mapped to the February 2009 human reference assembly (GRCh37/hg19). Positions in the coding regions of the reference (with 25 bp flanking) were classified as a variant if they had a read depth of >3 and a variant allele frequency of ≥20%. The variant reports were then converted into vcf files, which were uploaded to Cartagenia Bench Lab NGS (currently known as Alissa Interpret; Agilent Technologies, Santa Clara, CA) for filtering and subsequent analysis of variants of interest. All variants of interest were confirmed by Sanger sequencing.

Whole genome sequencing 100KGP individuals

Affected individuals and family members underwent whole genome sequencing as part of the 100KGP, as previously described (The National Genomic Research Library v5.1, Genomics England. https://doi.org/10.6084/m9.figshare.4530893.v7). The complete main study, rare disease cohort was interrogated for rare (Minor allele frequency <0.001, gnomAD v4.1 and 100KGP rare disease cohort) protein-altering variants in the *RPS4X* gene. Those identified in affected males were selected for further analysis, including interrogation of tiered variants for alternate diagnoses, AlphaMissense prediction of effect, segregation within included family members, captured human phenotype ontology (HPO) data and family history.

X-inactivation studies of Patient 1-2 family members

X-inactivation analysis of the Androgen Receptor (AR) locus was performed on genomic DNA extracted from peripheral blood. The X-inactivation pattern was determined by PCR analysis of a polymorphic CAG repeat in the first exon of the *AR* gene. Amplification of the *AR* gene both before and after digestion with the methylation-sensitive HpaII restriction enzyme was used to determine the methylation status of the both X chromosomes[14]. While this analysis measures whether inactivation of the X-chromosome is skewed toward one chromosome, it does not specifically inform the direction of skewed inactivation. The assumption is that the affected chromosome is selectively inactivated favoring expression from the wild type chromosome. However, without directly testing this we cannot confirm this possibility.

Zebrafish strains and animal husbandry

Animals were maintained according to standard protocols. The TLAB zebrafish strain was obtained from the Zebrafish International Resource Center (ZIRC, Eugene, OR). Embryonic staging was performed according to established criteria. In some cases 0.003% 1-phenyl 2-thiourea (PTU) was added to embryo medium to block pigmentation. Handling and euthanasia of fish complied with the policies of the Greenwood Genetic Center, as approved by the GGC's Institutional Animal Care and Use Committee (permit #A2022-01-003-Y3).

Methods for euthanasia

All larvae used in the study were euthanized according to nationally established guidelines and in accordance with the GGC PHS and IACUC-approved policies. In all cases, larvae were terminally anesthetized in a solution of Tris-buffered pharmaceutical grade MS-222.

Western blot of RPS4X abundance in patient cell lines

For Western blots, cells were lysed according to established protocols and analyzed by SDS PAGE. Fibroblasts were lysed in a Tris-Triton buffer (10mN Tris pH 7.4, 100 mM NaCl, 1 mM EDTA, 1% Triton X-100, 10% glycerol, 0.1% SDS, 0.5% deoxycholate) containing protease inhibitors. EBV-transformed lymphoblasts were lysed in a RIPA buffer plus protease inhibitors. Protein concentration was determined using the micro-BCA assay (Thermo Scientific, Waltham, MA, USA, cat#23235). Western blotting was performed using PVDF. The RPS4X primary antibody (abcam, ab211427) was used at 1:500. Blots were developed using the Clarity ECL system (BioRad, Hercules, CA, USA, cat#1705060) and imaged on a BioRad ChemiDoc imaging system. Densitometry was performed on Image J software. The equivalence of protein loading between lanes was normalized to total protein as assessed by Ponceau staining.

Quantitative PCR analyses of RPS4X and RPS4Y transcript abundance in patient cell lines

Quantitative RT-PCR was performed as previously described[15]. Total RNA was isolated from whole embryos and larvae using Direct-zol RNA microprep kit (Zymo Research) according to the manufacturer's instructions. An additional DNAse digestion step was added to ensure removal of genomic DNA. cDNA was synthesized using the qScript cDNA synthesis kit (Quanta Biosciences). Primers used for PCR amplification included: *RPS4X* Forward Primers 5' TTGGCAAGGGCAACAAACCA and 5' TGTCACCCAGGGACCCATTTC. RPS4X Reverse Primers 5' ACCTTG GATTTCCCTGCCCA and 5' CTGCTACTGCAATTTAGCCACTG Ribosomal protein L4 (*RPL4*) was used as an internal normalization control. Amplification reactions were performed using the PerfeCTa SYBR Green FastMix on a BioRad CFX96 real time system (BioRAd). Data were analyzed using the Prizm graphing program.

RPS4X DNA constructs

DNA constructs containing either wild type or the p.(Arg221Gln) variant version of zebrafish *rps4x* were commercially generated and cloned into the pCSII expression vector by GeneArt (ThermoFisher Life Sciences, Waltham, MA, USA).

Morpholino knockdown of rps4x expression in developing zebrafish

rps4x expression was inhibited in developing zebrafish using a morpholino (5' TCACAGAAGATCATTAAGCTCACCT 3') designed to the exon4-intron4 boundary (Gene Tools, LLC, Eugene, OR, USA). 1-cell stage embryos were injected with either 0.3 or 0.5 nL of 1 μM *rps4x* morpholino. The degree of inhibition was confirmed by RT-PCR analysis of *rps4x* abundance using primers to exon 3 and 7: exon 3 Forward 5'- AGG TCCGCACTGACATCAC-3' and exon 7 Reverse 5'- GCTCTGTT TGGCAGCCAGT-3'. The resulting transcripts were cloned by TA cloning and sequenced using primers targeting vector M13 sequences. Sequencing confirmed retention of intron 4 and a resulting introduction of several in-frame STOP codons. Analyses of genetic rescue was performed by injecting 120 pg of either wildtype or variant containing (p.Arg221Gln) *rps4x* zebrafish mRNA into a wild type or *rps4x* morphant background.

Microscopic analyses of BODIPY-labeled zebrafish embryos

For live analyses of the developing zebrafish brain, 1dpf animals were incubated overnight in embryo media containing 50 nM of Bodipy Ceramide (cat#D3861, ThermoFisher Sciences, Waltham, MA USA). Animals were mounted live in 0.8% agarose and imaged as previously described using a 40X water immersion objective (N.A.1.15) on an Olympus FV3000 laser scanning confocal microscope[16]. Maximum intensity projections were generated using the ImageJ software[17] and processed with Adobe PhotoShop (CS6).

Statistical analyses

In cases where numerical or quantitative data was generated standard error of the mean (S.E.M.) and a two-tailed Student's *t* test was used for statistical significance. Data was processed on GraphPad Prism (Version 7.0a). Larval gender is not established until later in development so is not a relevant consideration for these studies. No randomization was applied.

Protein structure modeling and analysis

We used MetaDome web server[18] to determine the protein tolerance landscape of human RPS4X.

Data availability

All data types presented in this paper will be shared by the lead contact upon request.

Received: 14 May 2025; Accepted: 14 April 2026;
Published online: 24 April 2026

References

1. Schwartz, C. E. et al. X-Linked intellectual disability update 2022. *Am. J. Med. Genet. A* **191**, 144–159 (2023).
2. Uechi, T., Tanaka, T. & Kenmochi, N. A complete map of the human ribosomal protein genes: assignment of 80 genes to the cytogenetic map and implications for human disorders. *Genomics*. **72**, 223–230 (2001).
3. Brooks, S. S. et al. A novel ribosomopathy caused by dysfunction of RPL10 disrupts neurodevelopment and causes X-linked microcephaly in humans. *Genetics*. **198**, 723–733 (2014).
4. Uliana, V. et al. Spectrum of X-lin ked intellectual disabilities AND psychiatric symptoms in a family harbouring a Xp22.12 microduplication encompassing the RPS6KA3 gene. *J Genet.* **98**, 10 (2019).
5. Noller, H. F. The ribosome comes to life. *Cell* **187**, 6486–6500 (2024).
6. Beavan, A. J. S. et al. Specialized ribosomes: integrating new insights and current challenges. *Philos. Trans. R. Soc. Lond. B Biol. Sci.* **380**, 20230377 (2025).
7. Shigeoka, T. et al. On-site ribosome remodeling by locally synthesized ribosomal proteins in axons. *Cell Rep.* **29**, 3605–3619 e3610 (2019).
8. Hamvas, R. M. et al. Rps4 maps near the inactivation center on the mouse X chromosome. *Genomics* **12**, 363–367 (1992).
9. Watanabe, M., Zinn, A. R., Page, D. C. & Nishimoto, T. Functional equivalence of human X- and Y-encoded isoforms of ribosomal protein S4 consistent with a role in Turner syndrome. *Nat. Genet* **4**, 268–271 (1993).
10. Sobreira, N., Schiettecatte, F., Valle, D. & Hamosh, A. GeneMatcher: a matching tool for connecting investigators with an interest in the same gene. *Hum. Mutat.* **36**, 928–930 (2015).
11. Dastidar, S. G. & Nair, D. A ribosomal perspective on neuronal local protein synthesis. *Front. Mol. Neurosci.* **15**, 823135 (2022).
12. Spellicy, C. J. et al. Three additional patients with EED-associated overgrowth: potential mutation hotspots identified? *J. Hum. Genet.* **64**, 561–572 (2019).
13. Klionsky, D. J. et al. Guidelines for the use and interpretation of assays for monitoring autophagy (4th edition)(1). *Autophagy* **17**, 1–382 (2021).
14. Allen, R. C., Zoghbi, H. Y., Moseley, A. B., Rosenblatt, H. M. & Belmont, J. W. Methylation of HpaII and HhaI sites near the polymorphic CAG repeat in the human androgen-receptor gene correlates with X chromosome inactivation. *Am. J. Hum. Genet.* **51**, 1229–1239 (1992).
15. Flanagan-Steet, H. et al. TGF-ss regulates cathepsin activation during normal and pathogenic development. *Cell Rep.* **22**, 2964–2977 (2018).
16. Flanagan-Steet, H., Fox, M. A., Meyer, D. & Sanes, J. R. Neuromuscular synapses can form in vivo by incorporation of initially aneural postsynaptic specializations. *Development* **132**, 4471–4481 (2005).
17. Lim, C. Y. et al. ER-lysosome contacts enable cholesterol sensing by mTORC1 and drive aberrant growth signalling in Niemann-Pick type C. *Nat. Cell Biol.* **21**, 1206–1218 (2019).
18. Wiel, L. et al. MetaDome: pathogenicity analysis of genetic variants through aggregation of homologous human protein domains. *Hum. Mutat.* **40**, 1030–1038 (2019).

Acknowledgements
The authors wish to thank the families for their participation in these studies. We also thank Cindy Skinner for her assistance with sample coordination for functional studies. We also acknowledge the staff of the Alin Aquaculture facility for the expert care of all animals used in this study. The study was supported by the Greenwood Genetic Center and its Genome Discovery Program. We also acknowledge that this research was made possible through access to data in the National Genomic Research Library, which is managed by Genomics England Limited (a wholly owned company of the Department of Health and Social Care). The National Genomic Research Library holds data provided by patients and collected by the NHS as part of their care and data collected as part of their participation in research. The National Genomic Research Library is funded by the National Institute for Health Research and NHS England. The Wellcome Trust, Cancer Research UK and the Medical Research Council have also funded research infrastructure. Functional analyses for this study were supported by the Greenwood Genetic Center.

Author contributions
R.E.S., M.F. and H.F.S. conceived the study. R.E.S. and K.C. saw I1 and I2. M.F. and R.L. identified the original *RPS4X* variants in individuals 1 and 2. S.B. and T.S. saw and reported variants for I3. E.W. and D.J. manage the care of I5, C.W. manages the care of I6. C.M.R., L.H., and P.N.L. performed experiments. G.A., R.A.S., and H.F.S. evaluated data, performed bioinformatic analyses and wrote the manuscript. All authors reviewed the manuscript.

Competing interests
The authors declare no competing interests.

Additional information
Supplementary information The online version contains supplementary material available at https://doi.org/10.1038/s41525-026-00573-0.

Correspondence and requests for materials should be addressed to Heather Flanagan-Steet.